

Search for the QCD Critical Point in High Energy Heavy-ion Collisions



Xiaofeng Luo (罗晓峰)

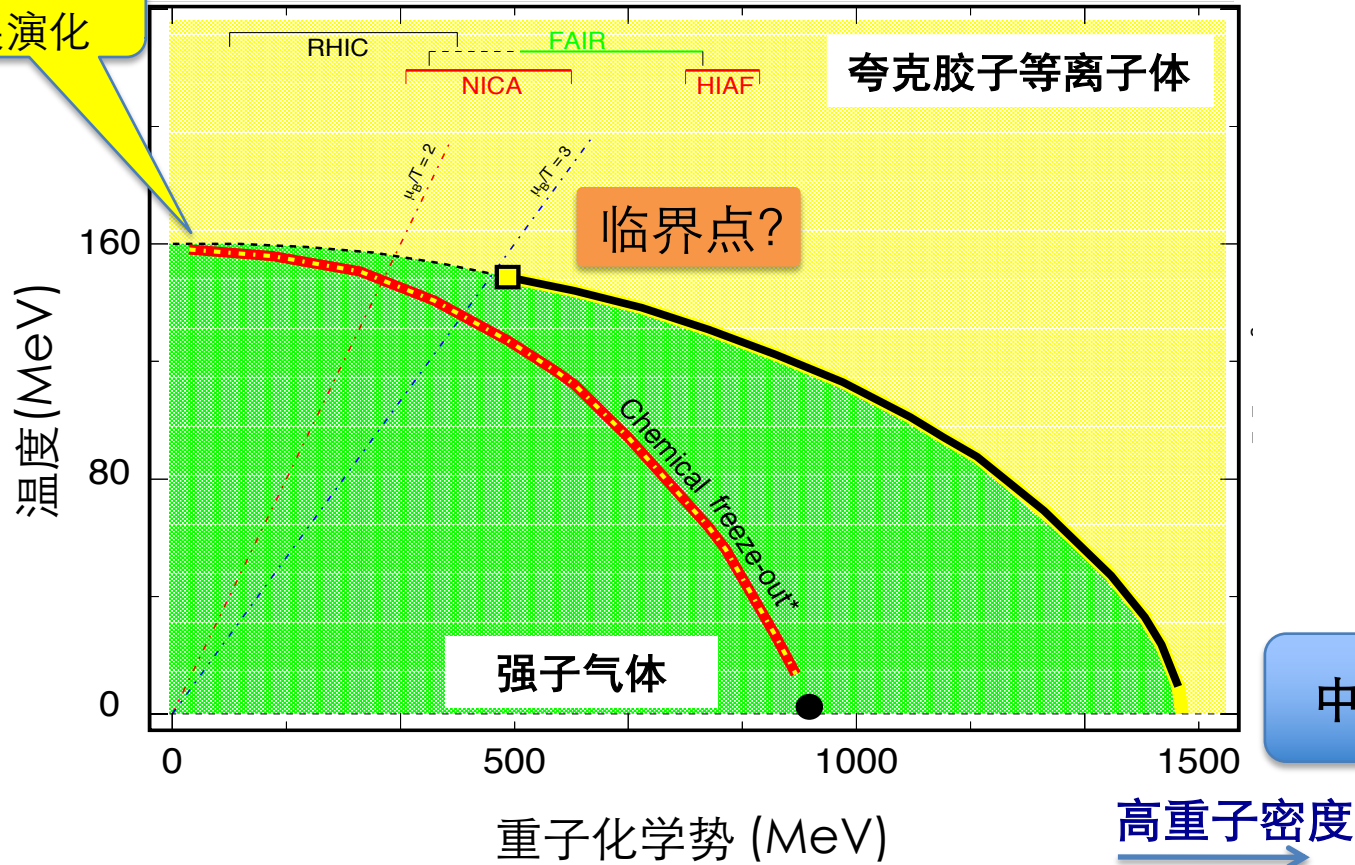
Central China Normal University





强相互作用 (QCD) 物质相图

早期宇宙
发展演化



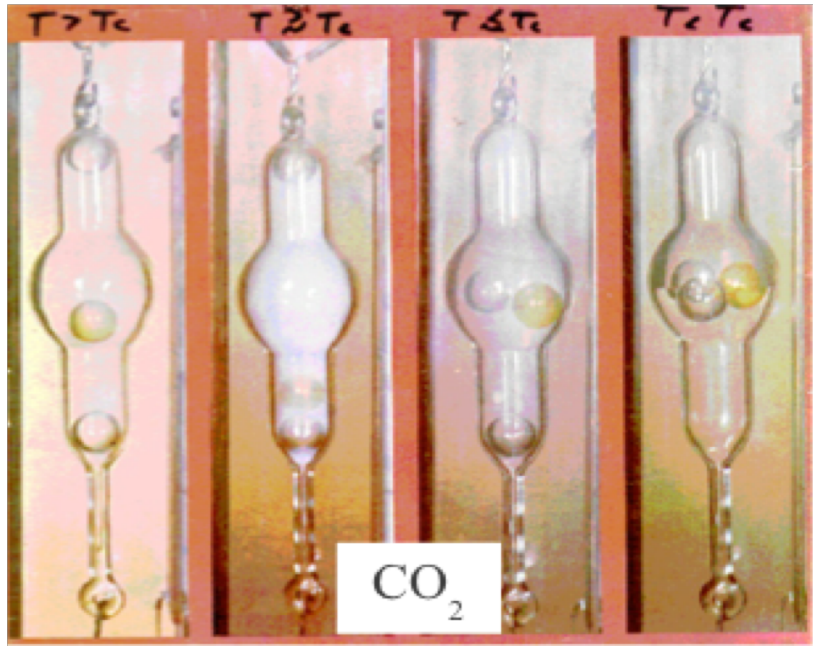
At $\mu_B=0$, smooth crossover
Y. Aoki, et al. Nature 443, 675 (2006)

重要科学问题: 是否存在QCD相变临界点及可能的位置?



Critical Point and Critical Phenomena

T. Andrews. Phil. Trans. Royal Soc., 159:575, 1869.



First CP is discovered in 1869 for CO₂ by Andrews.

$$T_c = 31^\circ\text{C}$$

Critical Phenomena :

- Large density fluctuations and long range correlation
- Divergence of Correlation length (ξ), Susceptibilities (χ), heat capacity (C_V), Compressibility (κ) etc. Critical opalescence.

Heavy-ion collisions:

- 1) Effects of finite time and size.
- 2) Non-equilibrium effects.



Location of CEP: Theoretical Prediction

➤ **Lattice QCD:**

1): Fodor&Katz, JHEP 0404,050 (2004):

$$(\mu_B^E, T_E) = (360, 162) \text{ MeV (Reweighting)}$$

2): Gavai&Gupta, NPA 904, 883c (2013)

$$(\mu_B^E, T_E) = (279, 155) \text{ MeV (Taylor Expansion)}$$

3): F. Karsch et al. NPA 956, 352 (2016).

$$(\mu_B^E / T_E > 2)$$

➤ **Dyson-Schwinger Equation (DSE):**

1): Y. X. Liu, et al., PRD90, 076006 (2014); 94, 076009 (2016). PRL

$$(\mu_B^E, T^E) = (372, 129) ; (262.3, 126.3) \text{ MeV} \\ (330, 128), L=2\text{fm} (450, 109)$$

2): Hong-shi Zong et al., JHEP 07, 014 (2014).

$$(\mu_B^E, T_E) = (405, 127) \text{ MeV}$$

3): C. S. Fischer et al., PRD90, 034022 (2014).

$$(\mu_B^E, T^E) = (504, 115) \text{ MeV}$$

➤ **Functional Renormalization Group (FRG):**

$$(\mu_B^E, T^E) = (635, 107) ; \text{Weijie Fu et al.}$$

$$(\mu_B^E, T^E) = (780, 55); \text{Defu Hou et al. PRD96 (2017)}$$

➤ **PNJL**, $(\mu_B^E, T^E) = (720, 90)$, Mei Huang, et al. EPJC 79, 245 (2019).

$$\mu_B^E = 262 \sim 780 \text{ MeV}, T_E = 55 \sim 162 \text{ MeV}$$

High Energy Nuclear Collision Experiments

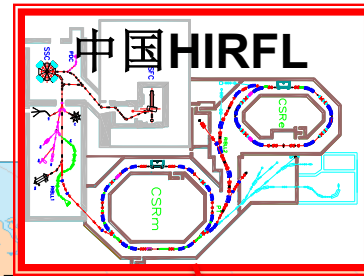
CEE@Lanzhou



美国RHIC



日内瓦LHC



中国HIRFL



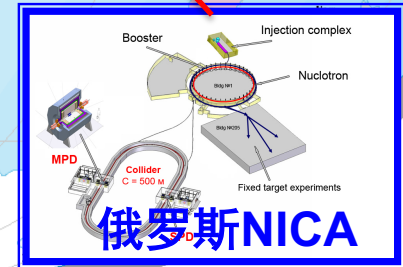
日本 JPARC-HI



十二五项目 HIAF 2023

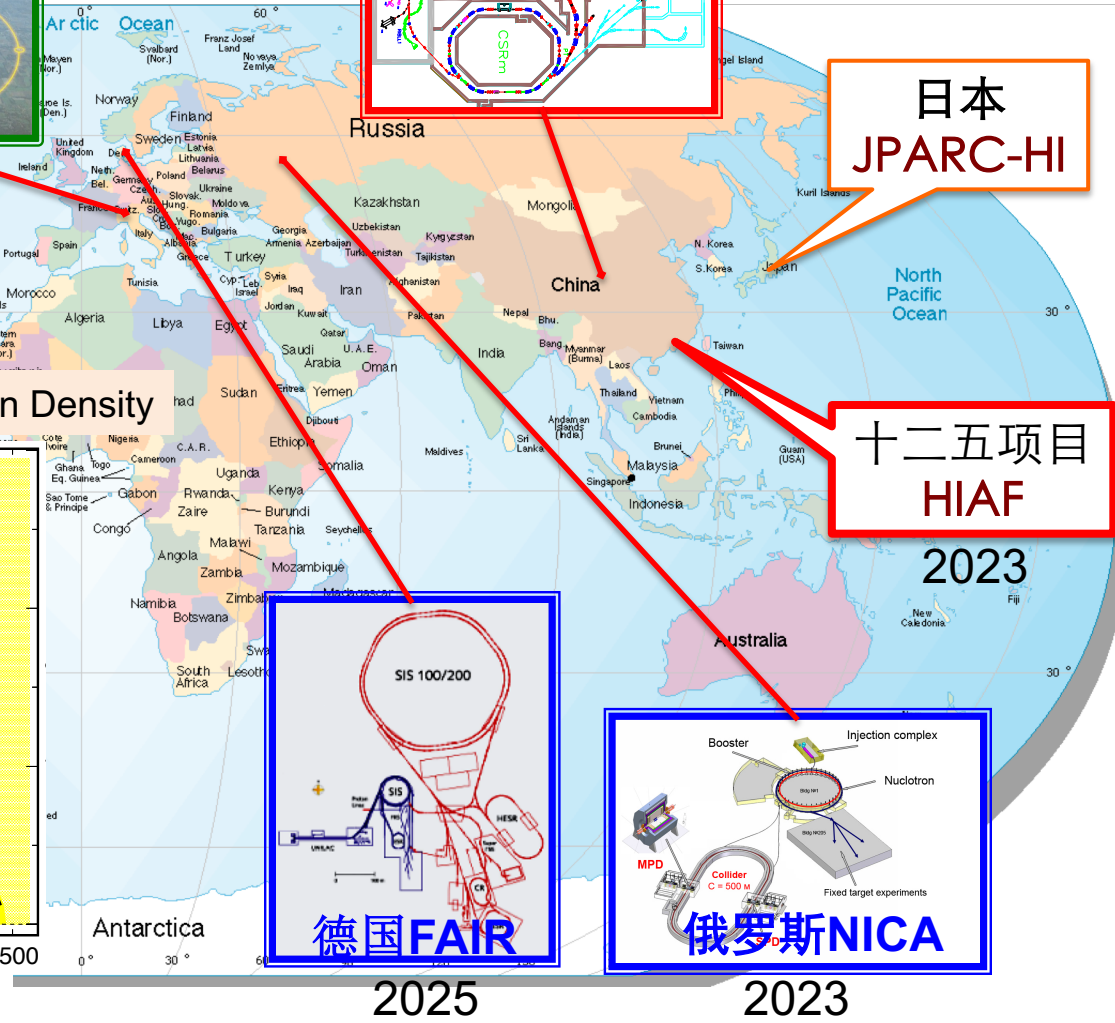
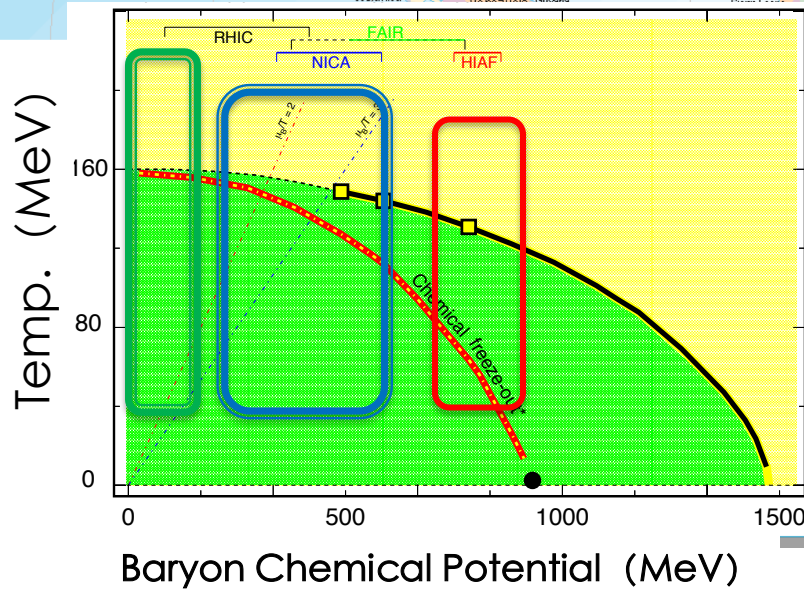


德国FAIR



俄罗斯NICA

Exploring QCD phase structure at High Baryon Density

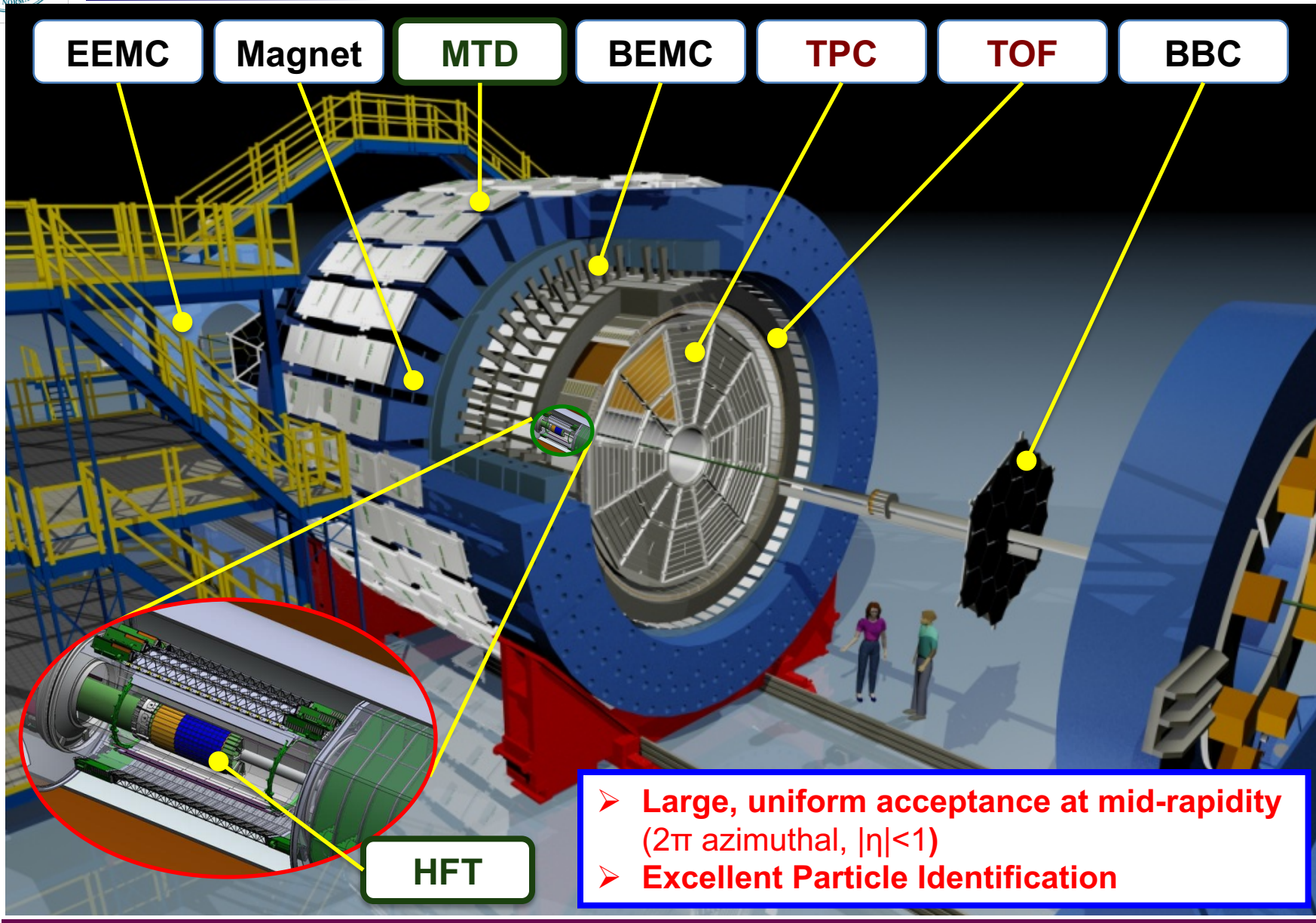


2025

2023



STAR Detector System

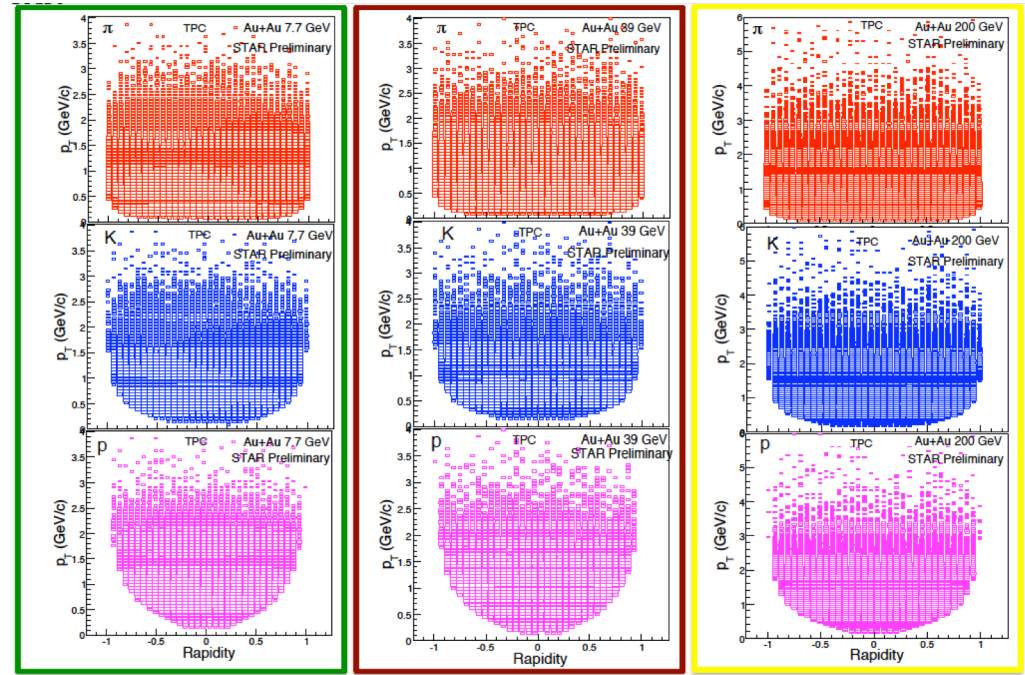




RHIC Beam Energy Scan Phase I (2010-2017)

$\sqrt{s_{NN}}$ (GeV)	Year	Events (10^6)	* μ_B (MeV)	* T_{CH} (MeV)
200	2010	238	25	166
62.4	2010	45	73	165
54.4	2017	1200	83	165
39	2010	86	112	164
27	2011	32	156	162
19.6	2011	15	206	160
14.5	2014	13	264	156
11.5	2010	7	316	152
7.7	2010	3	422	140

Uniform acceptance at Mid-rapidity



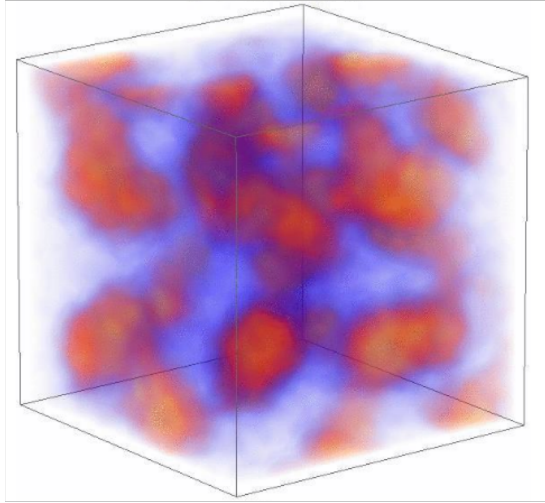
*(μ_B, T_{CH}) : J. Cleymans et al., PRC 73, 034905 (2006)

➤ Access the QCD phase diagram: vary collision energies/centralities.

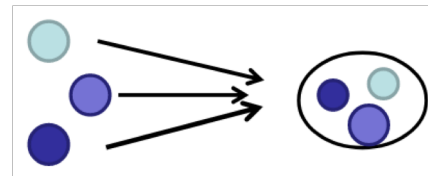
RHIC BES-I : $20 < \mu_B < 420$ MeV



Experimental Observables



In the vicinity of critical point
Large density fluctuations and long range corr.



From Feng Li

**Conserved charge
(B, Q, S) fluctuations**

**Baryon clustering:
light nuclei production**

Experimental Signatures:

Non-monotonic variation as a function of collision energy.

Caveats : finite size and time effect, non-critical physics contributions

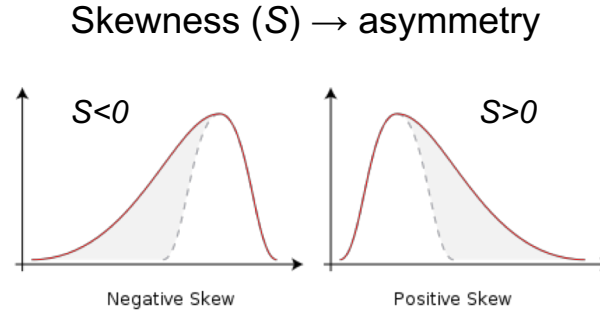


Higher Order Fluctuations of Conserved Quantities (B, Q, S)

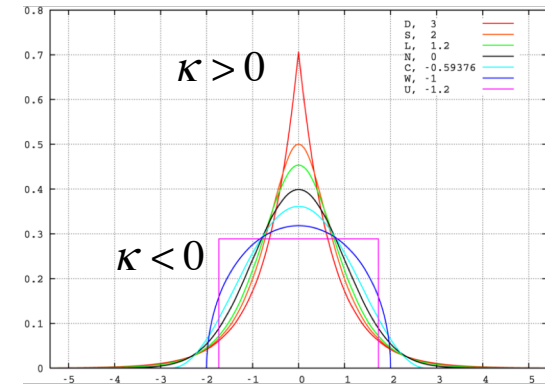
1. Higher order cumulants/moments: describe the shape of distributions and quantify fluctuations. (sensitive to the correlation length (ξ))

$$\begin{aligned} \langle \delta N \rangle &= N - \langle N \rangle \\ C_1 &= M = \langle N \rangle \\ C_2 &= \sigma^2 = \langle (\delta N)^2 \rangle \\ C_3 &= S\sigma^3 = \langle (\delta N)^3 \rangle \\ C_4 &= \kappa\sigma^4 = \langle (\delta N)^4 \rangle - 3 \langle (\delta N)^2 \rangle^2 \end{aligned}$$

$$\langle (\delta N)^3 \rangle_c \approx \xi^{4.5}, \quad \langle (\delta N)^4 \rangle_c \approx \xi^7$$



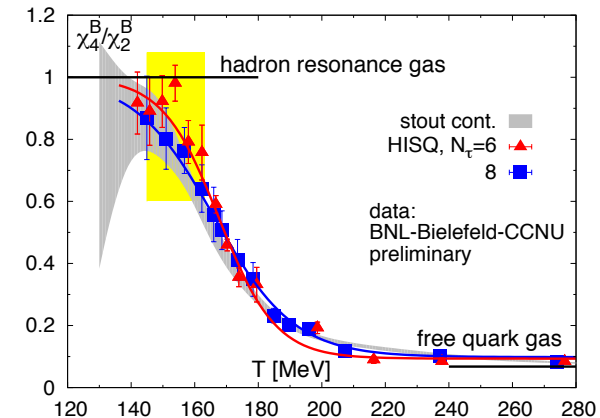
Kurtosis (κ) → Sharpness



M. A. Stephanov, *Phys. Rev. Lett.* 102, 032301 (2009); 107, 052301 (2011).
M. Asakawa, S. Ejiri and M. Kitazawa, *Phys. Rev. Lett.* 103, 262301 (2009).

2. Direct connect to the susceptibility of the system

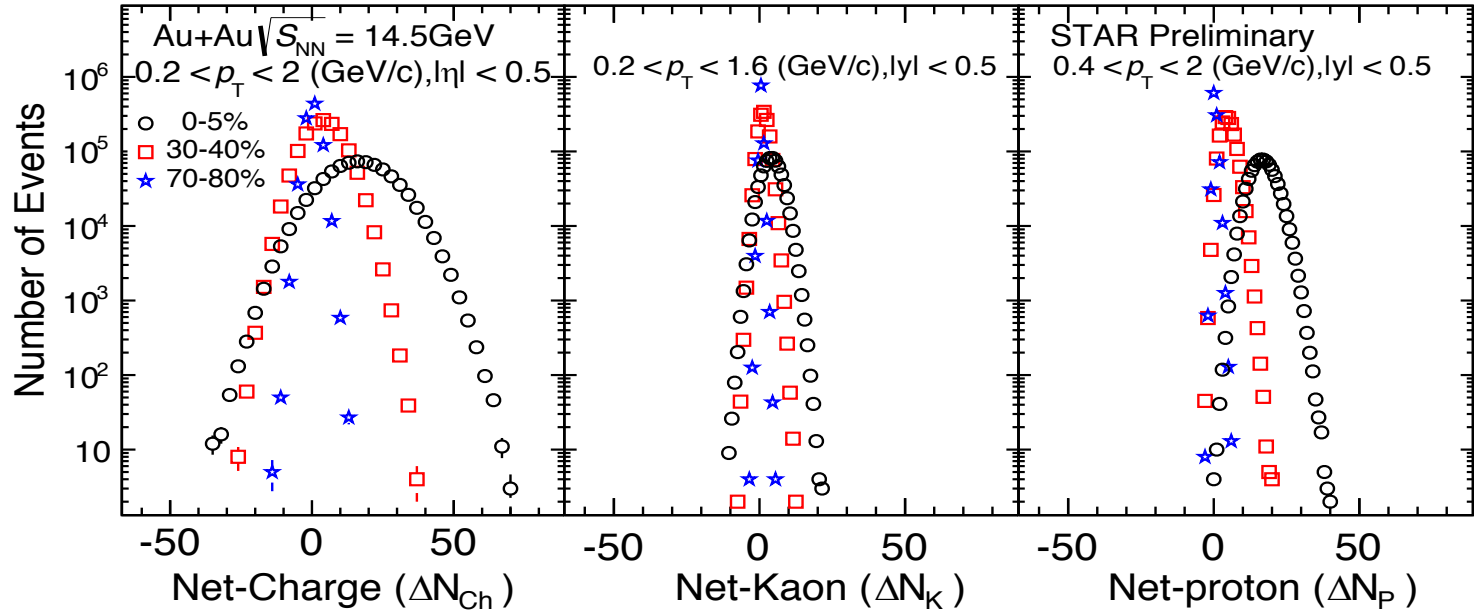
$$\begin{aligned} \frac{\chi_q^4}{\chi_q^2} &= \kappa\sigma^2 = \frac{C_{4,q}}{C_{2,q}} & \frac{\chi_q^3}{\chi_q^2} &= S\sigma = \frac{C_{3,q}}{C_{2,q}}, \\ \chi_q^{(n)} &= \frac{1}{VT^3} \times C_{n,q} = \frac{\partial^n (p/T^4)}{\partial (\mu_q)^n}, q = B, Q, S \end{aligned}$$



Cheng et al, *PRD* (2009) 074505. F. Karsch and K. Redlich, *PLB* 695, 136 (2011).
S. Gupta, et al., *Science*, 332, 1525(2012). A. Bazavov et al., *PRL* 109, 192302(12) // S. Borsanyi et al., *PRL* 111, 062005(13)



Observables measured at STAR experiment



1. Statistical errors estimation : Delta theorem or bootstrap
2. Avoid auto-correlation effects: New centrality definition.
3. Suppress volume fluctuation: Centrality bin width correction (CBWC)
4. Detector efficiency correction : Binomial model

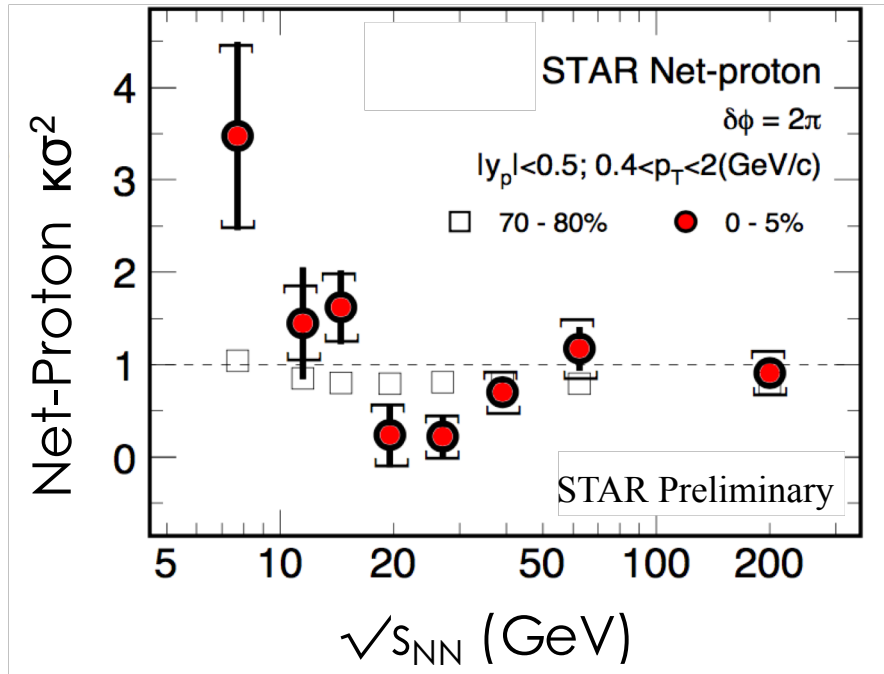
- **Net-Proton:** $N_p - N_{\bar{p}}$
(Net-Baryon, B)
- **Net-Charge:** $N_{Q^+} - N_{Q^-}$
- **Net-Kaon:** $N_{K^+} - N_{K^-}$
(Net-Strangeness, S)

Review Article : X. Luo and N. Xu, Nucl. Sci. Tech. 28, 112 (2017).

X.Luo, et al. J. Phys. G39, 025008 (2012); A. Bzdak and V. Koch, PRC86, 044904 (2012); X.Luo, et al. J. Phys. G40, 105104(2013); X.Luo, Phys. Rev. C 91, 034907 (2015); A. Bzdak and V. Koch, PRC91, 027901 (2015). T. Nonaka et al., PRC95, 064912 (2017). M. Kitazawa and X. Luo, PRC96, 024910 (2017). X. Luo and T. Nonaka, PRC99, 044917 (2019);

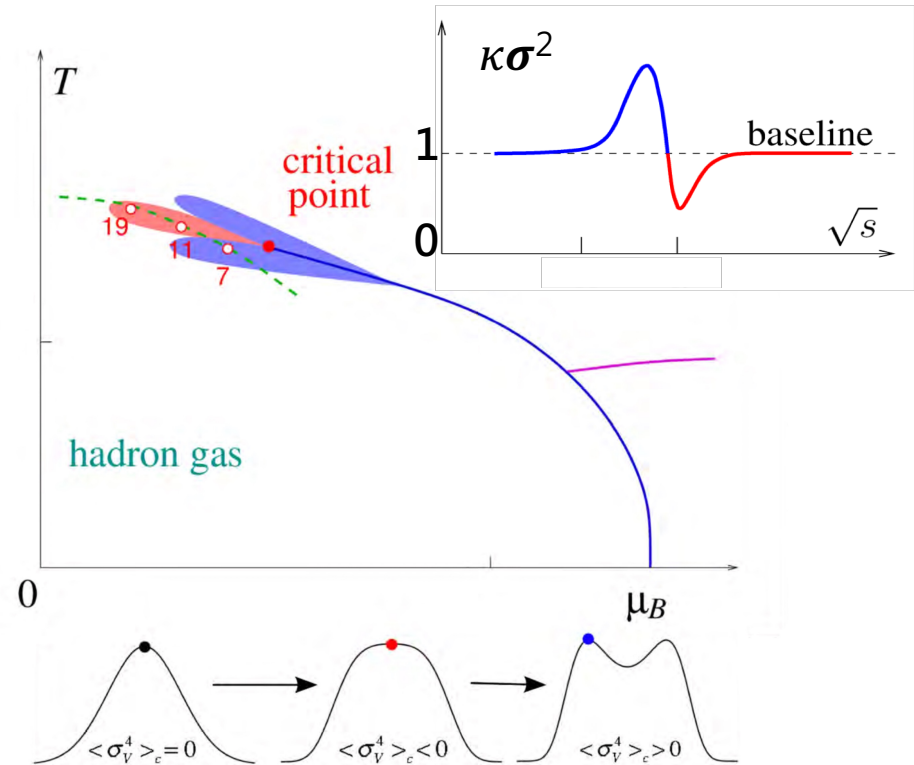
$$\kappa\sigma^2 = C_4/C_2$$

Experimental Measure



STAR: Phys. Rev. Lett. 105, 022302 (2010).
 Phys. Rev. Lett. 112, 032302 (2014).
 PoS CPOD2014 (2015) 019.

A theoretical calculation

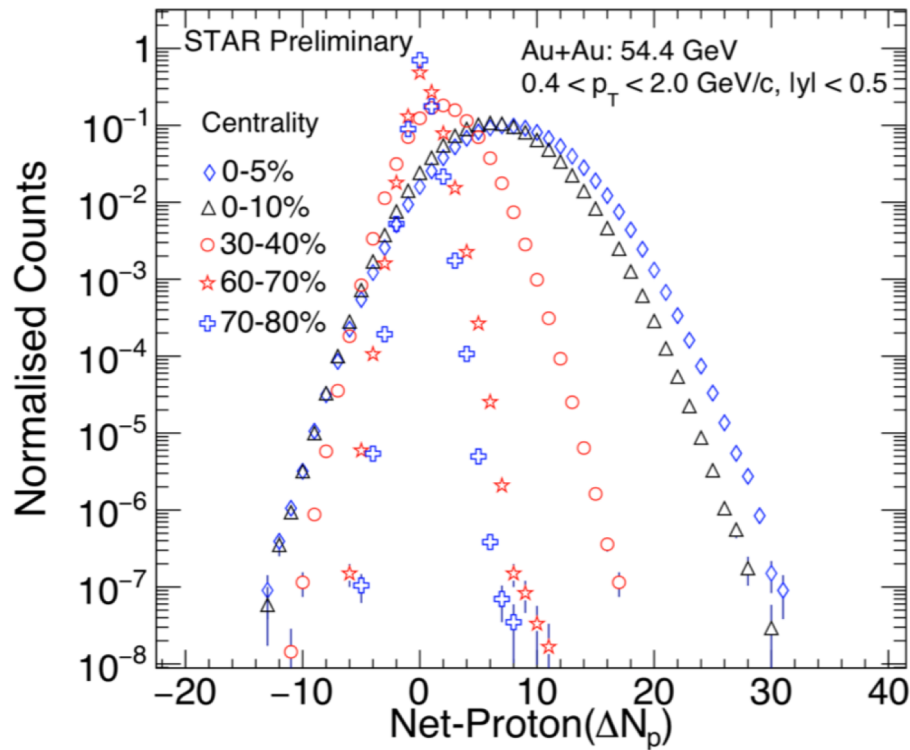


M. Stephanov, PRL107, 052301(2011); J. Phys. G: 38, 124147 (2011). Schaefer, Wanger, PRD 85, 034027 (2012) JW Chen, J. Deng et al., PRD93, 034037 (2016); PRD95, 014038 (2017).

- First observation of the non-monotonic energy dependence of fourth order net-proton fluctuations. **Hint of entering Critical Region ?**

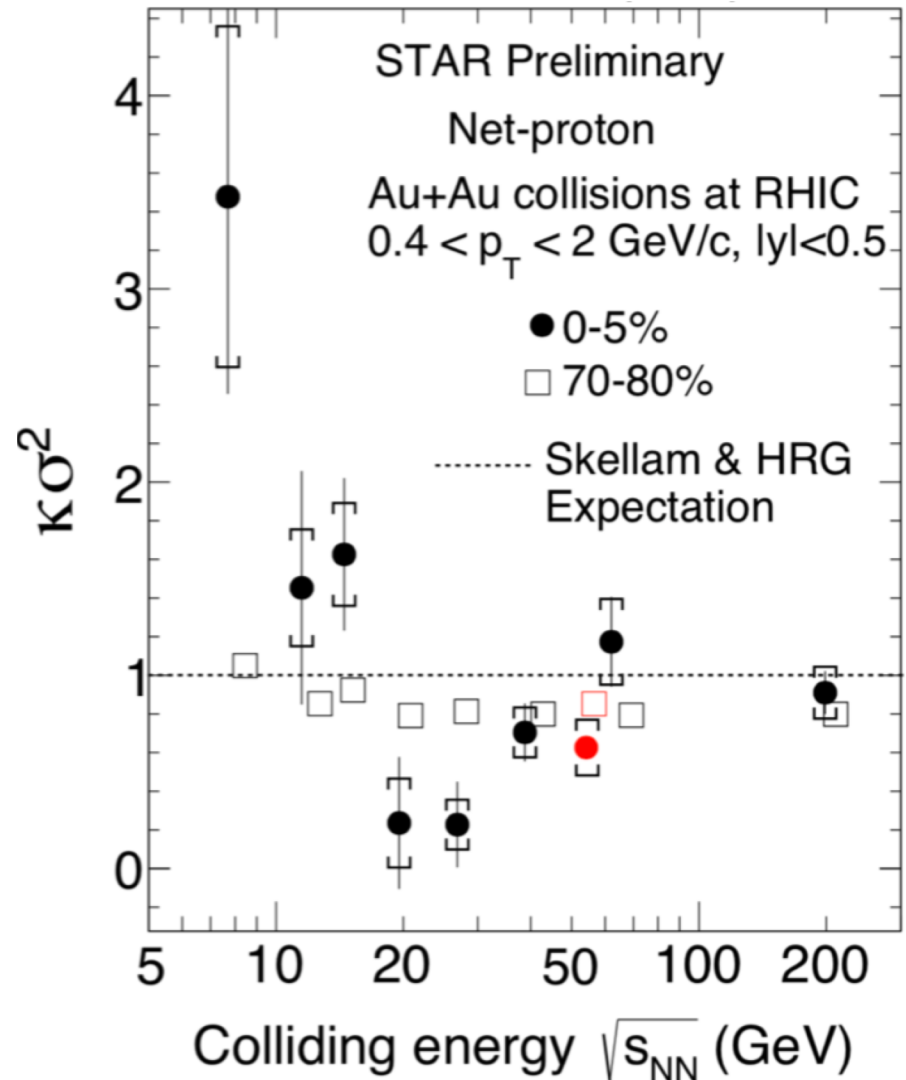


New data set : 54.4 GeV (2017)

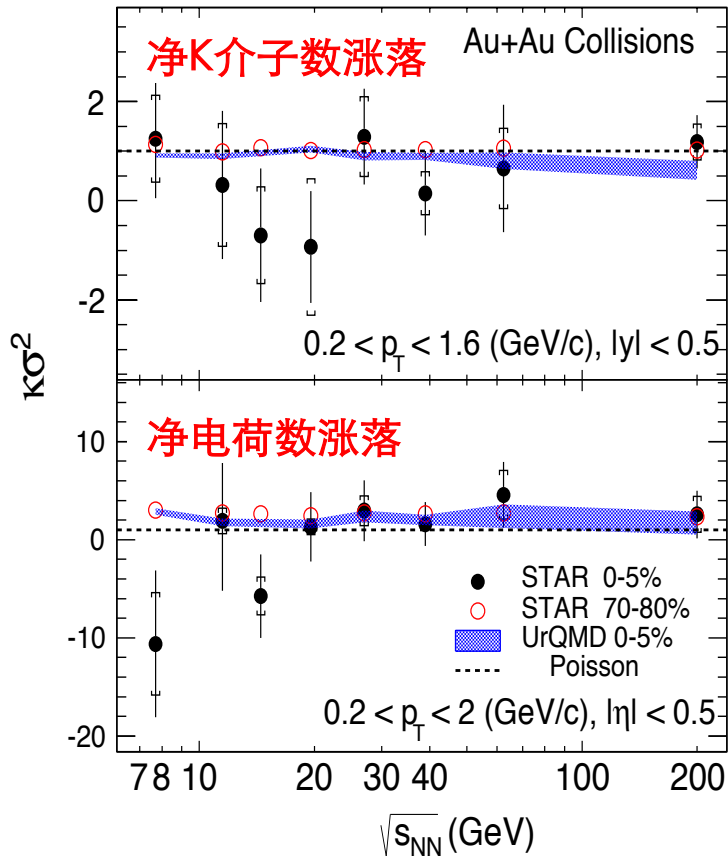


STAR, SQM 2019

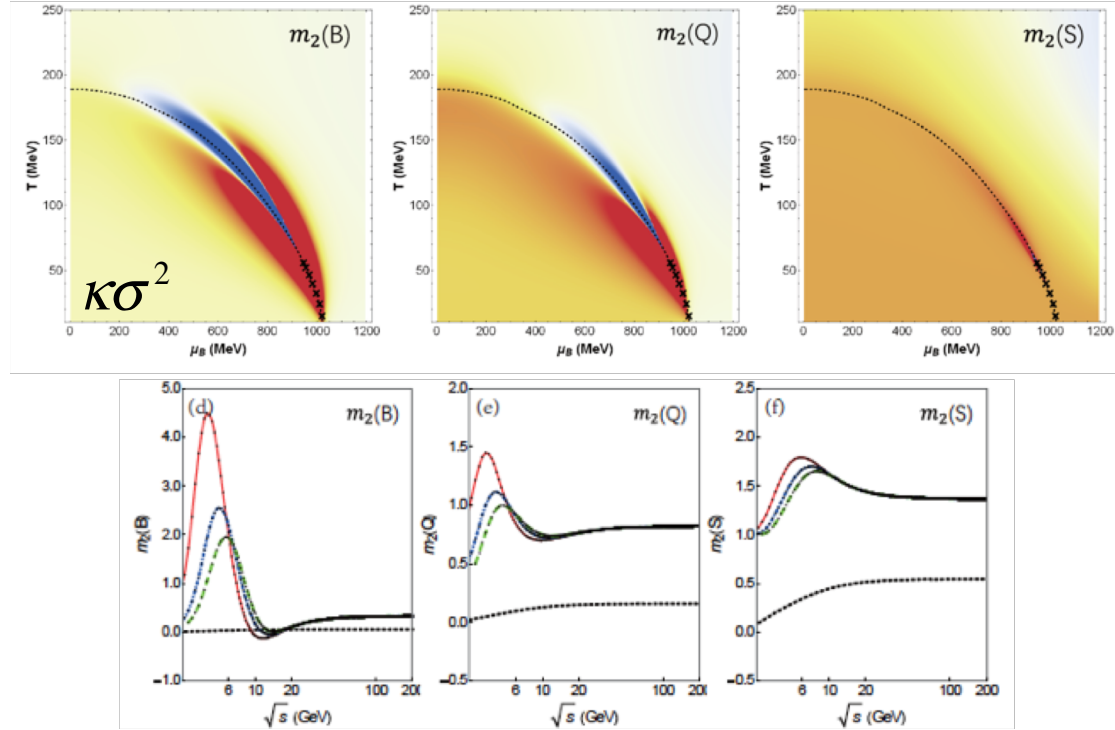
➤ Results at 54.4 GeV follow the trend well.



实验测量



理论模型(NJL)计算



临界信号强度：净重子>净电荷>净奇异数
 (由于奇异夸克质量远大于u,d夸克质量, $m_s \gg m_{u,d}$)
 W. Fan, X. Luo, H.S. Zong, IJMPA 32, 1750061 (2017).

净K介子: STAR, Phys. Lett. B 785, 551 (2018)
 净电荷: STAR, Phys. Rev. Lett. 113, 092301 (2014)

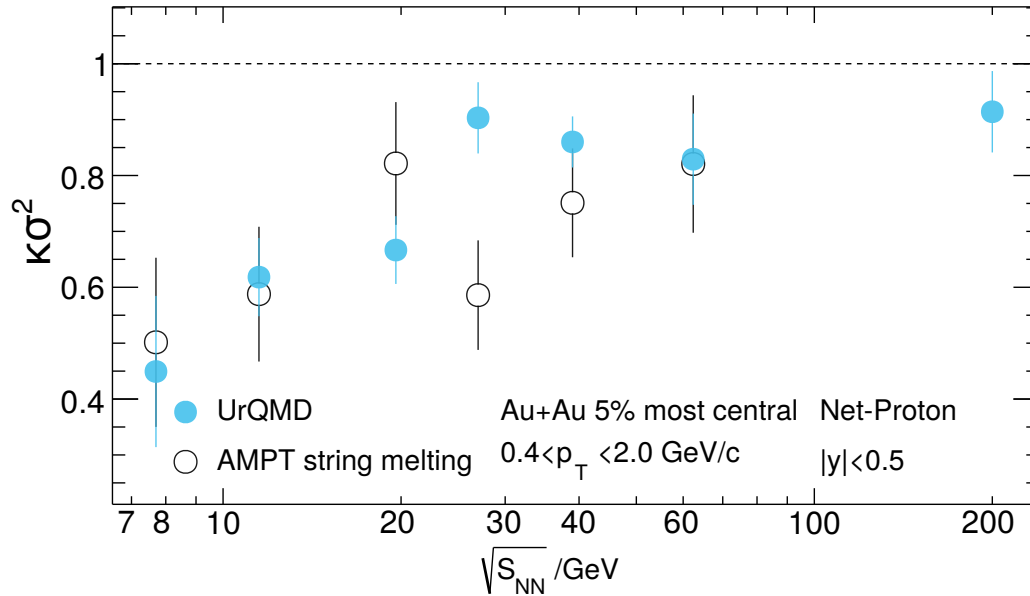
统计误差较大, 需要更高统计量进行精确测量

$$error(\kappa\sigma^2) \propto \frac{\sigma^2}{\varepsilon^2} \frac{1}{\sqrt{N_{evts}}}$$



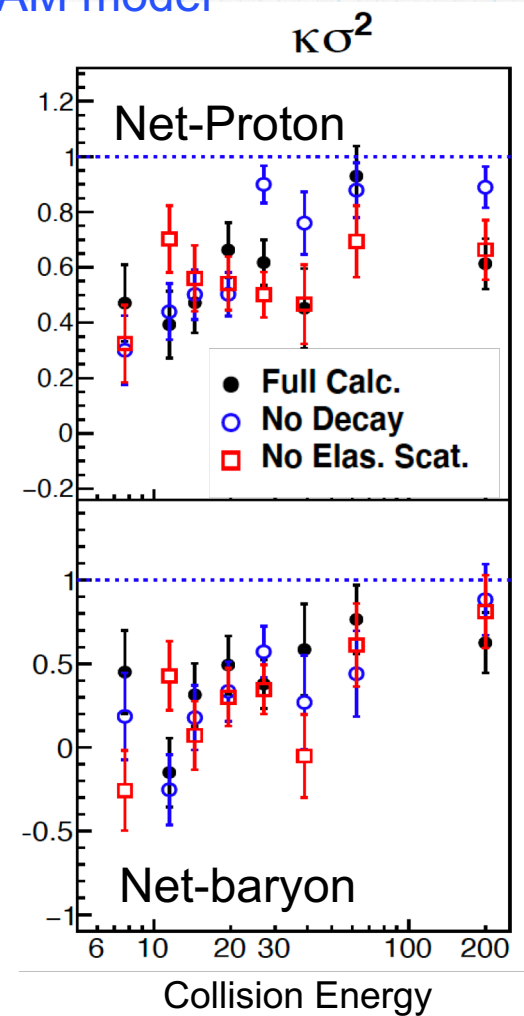
Non-critical Contributions: Transport Model Studies

UrQMD and AMPT models



- Transport model (no CP physics) results show monotonic energy dependence: baryon number conservations
- Effects of weak decay and hadronic scattering are small

JAM model

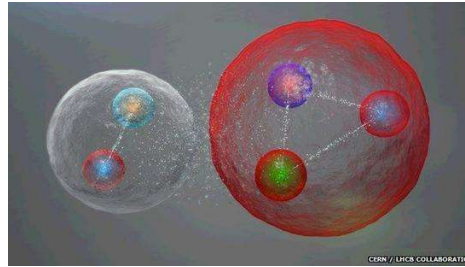


Z. Feckova, et al., PRC92, 064908(2015). J. Xu, et al., PRC94, 024901(2016). X. Luo et al., NPA931, 808(14), P.K. Netrakanti et al. 1405.4617, NPA947, 248(2016), P. Garg et al. PLB 726, 691(2013). S. He, et. al., PLB762, 296 (2016). S. He, X. Luo, PLB 774, 623 (2017).

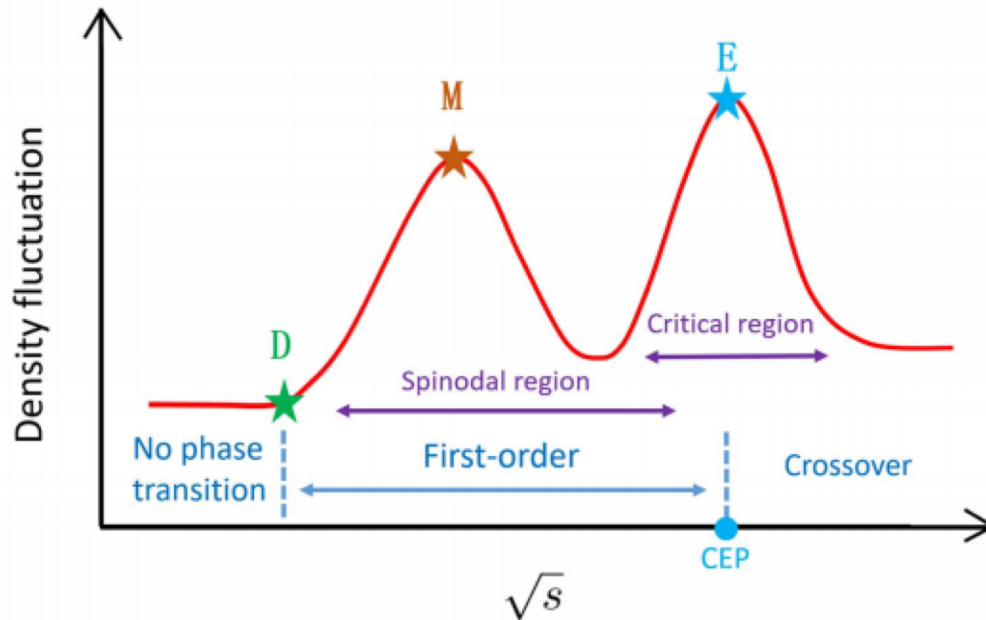


Probe the QCD phase structure with Light Nuclei

Near CP or 1st order phase transition, baryon density fluctuation become large.



Light nuclei production
(Baryon Clustering)



Coalescence + nucleon density flu.

$$N_d = \frac{3}{2^{1/2}} \left(\frac{2\pi}{m_0 T_{\text{eff}}} \right)^{3/2} N_p \langle n \rangle (1 + \alpha \Delta n),$$

$$N_{3H} = \frac{3^{3/2}}{4} \left(\frac{2\pi}{m_0 T_{\text{eff}}} \right)^3 N_p \langle n \rangle^2 [1 + (1 + 2\alpha) \Delta n],$$

$$N_t \cdot N_p / N_d^2 \approx g(1 + \Delta n)$$

Neutron density fluctuations:

$$\Delta n = \langle (\delta n)^2 \rangle / \langle n \rangle^2$$

K. J. Sun, L. W. Chen, C. M. Ko, Z. Xu, Phys. Lett. B774, 103 (2017).

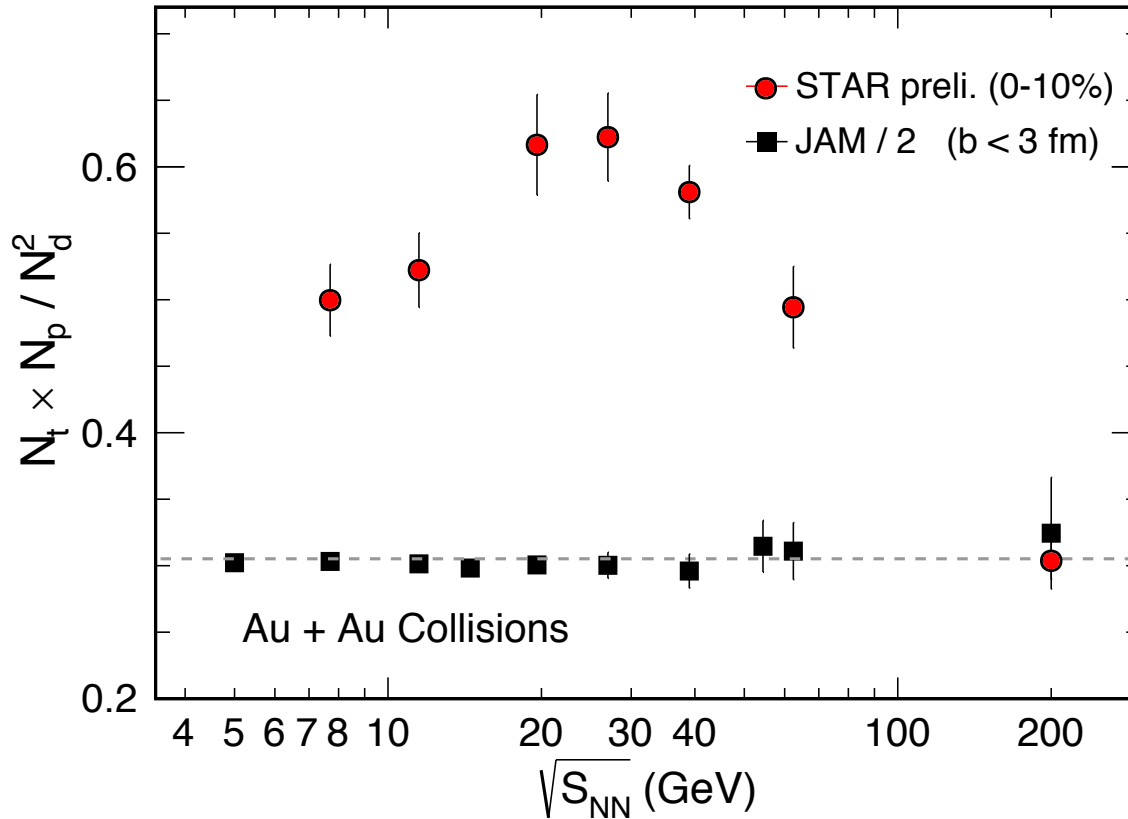
K. J. Sun, L. W. Chen, C. M. Ko, J. Pu, Z. Xu, Phys. Lett. B781, 499 (2018).

Edward Shuryak and Juan M. Torres-Rincon, Phys. Rev. C 100, 024903 (2019)



实验测量三：轻核产额比 ($N_p N_t / N_d^2$)

STAR(0-10%) vs. JAM(b<3fm)



氘 : Deuteron (d)
氚 : Triton (t)

$$N_t \cdot N_p / N_d^2 \approx g(1 + \Delta n)$$

$$g=0.29$$

Yield ratio is related to neutron density fluctuations

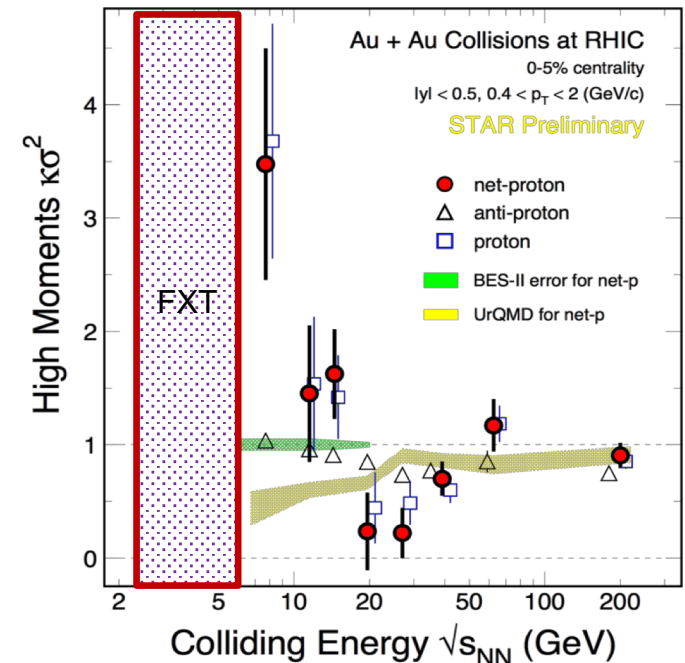
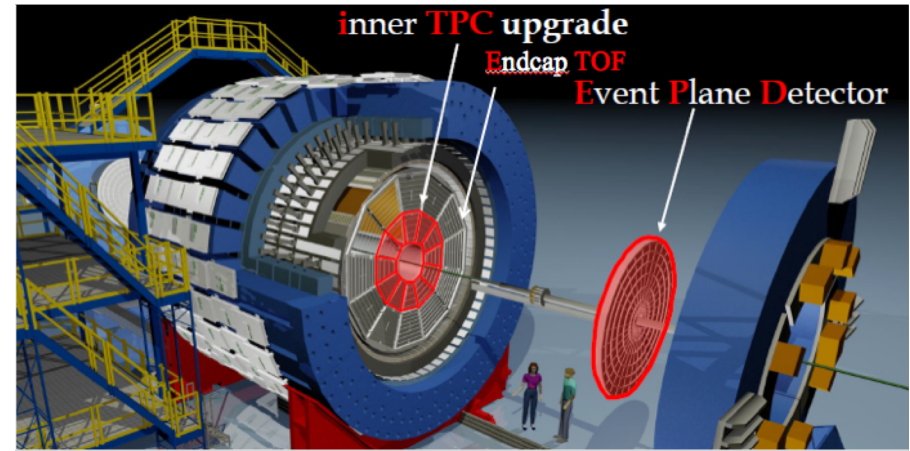
H. Liu et al, arXiv: 1909. 09304

- Yield ratios show a non-monotonic energy dependence with a peak around 20-30 GeV.
- Flat energy dependence of yield ratio observed in JAM model and cannot describe the data.



BES-II at RHIC (2019-2021)

$\sqrt{s_{NN}}$ (GeV)	Events (10^6)	BES II / BES I
19.6	400	2019 / 2011
14.5	300	2019 / 2014
11.5	230	2020 / 2010
9.2	160	2020 / 2008
7.7	100	2021 / 2010
17.1	250	2021



- BES-II : 10-20 times higher statistics than BES-I.
- FIX-target mode : $\sqrt{s_{NN}} = 3-7.7$ GeV (2018-2020).
- iTPC, ETOF, EPD upgrade completed.

- **Enlarge Acceptance** : η coverage from 1.0 to 1.5
- **Improve dE/dx and forward PID**
- **Improve centrality/event plane determination**



Summary and Outlook

- Fourth order net-proton fluctuations (C_4/C_2) in central Au+Au collisions shows non-monotonic energy dependence, with a minimum around 20-30 GeV.
- Light nuclei yield ratio in 0-10% central Au+Au collisions shows non-monotonic energy dependence with a peak around 20-30 GeV.
- Transport model simulation (No CP) show monotonic energy dependence.
- Study the QCD phase structure at **high baryon density** with **high precision**:
 - (1) BES-II at RHIC (2019-2021, both collider and fix target mode).
 - (2) Higher baryon density : CBM, NICA, CEE, JPARC.

Stay tuned for RHIC BES-II (2019-2021) !



Thank you!



2019-2021: BES II at RHIC

$\sqrt{s_{NN}}$ (GeV)	Events (10^6)	BES II / BES I	μ_B (MeV)	T_{CH} (MeV)
200	238	2010	25	166
62.4	46	2010	73	165
54.4	1000	2017	90	165
39	86	2010	112	164
27	30 (1000)	2011(2018)	156	162
19.6	400 / 15	2019 / 2011	206	160
14.5	300 / 13	2019 / 2014	264	156
11.5	230 / 7	2020 / 2010	315	152
9.2	160 / 0.3	2020 / 2008	355	140
7.7	100 / 3	2021 / 2010	420	140
17.1	250	2021	235	

Precise mapping the QCD phase diagram **$200 < \mu_B < 420\text{MeV}$**